Rare Metal Materials and Engineering
Volume 54, Issue 12, December 2025
Available online at www.rmme.ac.cn

Science Press

Cite this article as: Li Yuanjie, Zhao Yuqing, Liang Chenyu. Effect of Oxygen/Ar Flow Rate Ratio on Properties of Amorphous Ga_2O_3 Thin Films on Flexible and Rigid Substrates[J]. Rare Metal Materials and Engineering, 2025, 54(12): 2993-2999. DOI: https://doi.org/10.12442/j.issn.1002-185X.20240726.

ARTICLE

Effect of Oxygen/Ar Flow Rate Ratio on Properties of Amorphous Ga_2O_3 Thin Films on Flexible and Rigid Substrates

Li Yuanjie[1], Zhao Yuqing[1], Liang Chenyu[2]

[1] Key Laboratory for Physical Electronics and Devices, Ministry of Education, School of Electronic Science and Engineering, Xi'an Jiaotong University, Xi'an 710049, China; [2] Analytical & Testing Center, Xi'an Jiaotong University, Xi'an 710049, China

Abstract: Amorphous Ga_2O_3 (a-Ga_2O_3) thin films were prepared on flexible polyimide, rigid quartz glass, and Si substrates via radio frequency magnetron sputtering at room temperature. The effect of oxygen/Ar flow rate ratio on the structure, optical property, surface morphology, and chemical bonding properties of the a-Ga_2O_3 films was investigated. Results show that the average optical transmittance of the a-Ga_2O_3 films is over 80% within the wavelength range of 300–2000 nm. The extracted optical band gap of the a-Ga_2O_3 films is increased from 4.97 eV to 5.13 eV with the increase in O_2/Ar flow rate ratio from 0 to 0.25, due to the decrease in concentration of oxygen vacancy defects in the film. Furthermore, the optical refractive index and surface roughness of the a-Ga_2O_3 films are optimized when the O_2/Ar flow rate ratio reaches 0.25. X-ray photoelectron spectroscopy analysis also shows that the proportion of oxygen vacancies (V_O) and Ga-O chemical bonds in the O 1s peak is gradually decreased with the increase in O_2/Ar flow rate ratio from 0 to 0.25, proving that increasing the O_2/Ar flow rate ratio during film growth can reduce the concentration of oxygen vacancy defects in a-Ga_2O_3 films. In this case, a-Ga_2O_3 with optimal properties can be obtained. This work provides a research basis for high-performance flexible and rigid deep ultraviolet solar-blind detection devices based on a-Ga_2O_3 films.

Key words: solar-blind DUV photodetector; amorphous Ga_2O_3 thin film; flexible electronics; oxygen vacancy defect; RF magnetron sputtering

1 Introduction

Deep ultraviolet (DUV) spectra of wavelength between 200 and 280 nm are mostly absorbed by the ozone layer within the atmosphere from the sun to the Earth surface. Accordingly, no ultraviolet light of wavelength below 280 nm can be detected against the surrounding light background on Earth. This solar-blind photodetection technique has attracted considerable interest due to higher sensitivity, lower false alarm rate, and stronger anti-interference ability[1–5]. The development of the solar-blind ultraviolet photodetectors exhibits important applications in secure optical communication, ozone hole detection, and space exploration[6–8]. Recently, DUV photodetectors based on flexible substrates are expected to satisfy the increasing demands for next-generation portable robust electronics[9–11]. The lightweight feature and low cost of the flexible DUV photodetectors show advantages for versatile applications and large-scale uniform production.

Wide bandgap semiconductors, including AlGaN, ZnMgO, Ga_2O_3, and diamond, are widely used to fabricate high-performance DUV photodetectors[12–15]. Compared with other materials, Ga_2O_3 demonstrates attractive potentials in solar-blind photodetection because of its intrinsically ultrawide bandgap (about 4.9 eV) and the necessity of an alloying process[16–17]. Attention has been paid to the crystalline β-Ga_2O_3-based DUV photodetectors on single-crystal rigid substrates at high growth rate or high annealing temperature (>600 °C). Nevertheless, the crystalline Ga_2O_3 is not suitable for large-scale flexible electronics due to high synthesis temperature, inferior stability, and complex growth

Received date: December 12, 2024
Foundation item: Research Project of Shenzhen Science and Technology Innovation Committee (JCYJ20180306170801080)
Corresponding author: Li Yuanjie, Ph. D., Associate Professor, Key Laboratory for Physical Electronics and Devices, Ministry of Education, School of Electronic Science and Engineering, Xi'an Jiaotong University, Xi'an 710049, P. R. China, Tel: 0086-29-82664974, E-mail: liyuanjie@mail.xjtu.edu.cn

procedures. Recent research on development of DUV photodetectors using amorphous Ga_2O_3 (a-Ga_2O_3) has shown excellent ultraviolet sensitivity and a low dark current level. Arora et al[18] fabricated self-biased DUV photodetectors based on a-Ga_2O_3 thin films on paper substrates at room temperature. The photodetector exhibits high responsivity of 3.1 mA/W and external quantum efficiency (EQE) of 2.5% with a large intensity ratio I_{photo}/I_{dark} of 10^4 at zero bias. Han et al[19] studied the effect of Ar growth pressure on the performance of room temperature-deposited a-Ga_2O_3 DUV detectors[19]. A high-response a-Ga_2O_3-based DUV detector was realized at 0.5 Pa, and the maximum response of the device reached 436.3 A/W under ultraviolet light (240 nm) at bias of 25 V. In addition, Wang et al[20] reported high-performance a-Ga_2O_3-based avalanche photodetectors with specific detectivity of 1.8×10^{14} J (unit: Jones) and EQE of 2.9×10^7%. The mechanism of the intrinsic carrier transport and modified band alignment at the a-Ga_2O_3/ITO heterojunction was analyzed to explain these superior characteristics. Until now, most studies about the a-Ga_2O_3 based DUV photodetectors are focused on the improvement of DUV detectors. It is well believed that persistent photoconductivity (PPC) effect in oxides greatly slows down the detector response speed. Lany et al[21] developed a validated oxygen vacancy (V_O) defect model from first-principles calculations, which leads to PPC effect in metal oxides. The modulation of ambient oxygen pressure during the growth of a-Ga_2O_3 films plays an important role in controlling the intrinsic V_O defect density in a-Ga_2O_3. Therefore, a thorough and systematic investigation into the effects of ambient oxygen pressure on the properties of a-Ga_2O_3 films remains indispensable and urgent.

In this research, a-Ga_2O_3 thin films are deposited on flexible polyimide (PI), rigid quartz, and rigid silicon substrates using radio frequency (RF) magnetron sputtering at room temperature. The effect of the O_2/Ar flow rate ratio on the structure, optical property, surface morphology, and chemical bonding properties of the a-Ga_2O_3 films was discussed. Additionally, the mechanism of variations in optical bandgap and refractive index of the a-Ga_2O_3 films was analyzed with the increase in O_2/Ar flow rate ratio during film growth. The relationship between oxygen vacancy defect control and optimization of the a-Ga_2O_3 film properties was elucidated.

2 Experiment

The a-Ga_2O_3 thin films were deposited on flexible PI, rigid quartz glass, as well as rigid Si substrate via RF magnetron sputtering (Explorer, Denton Vacuum) under various oxygen flow rates at room temperature. Both flexible and rigid substrates were ultrasonically cleaned in acetone, methanol, and deionized water for 10 min and then dried using N_2 before film deposition. A high-purity, undoped Ga_2O_3 (99.99%) ceramic target was used as the sputter target. A low sputtering power of 150 W was applied to reduce the excessive ion bombardment damage on the flexible PI substrate. The a-Ga_2O_3 films with a thickness of 400 nm were obtained on both flexible and rigid substrates after magnetron sputtering deposition for 1 h. During the growth of a-Ga_2O_3 films, O_2 with flow rates of 0, 2, 3, 4, and 5 mL/min was introduced into the chamber while fixed Ar flow rate of 20 mL/min. Correspondingly, the O_2/Ar flow rate ratio was 0, 0.10, 0.15, 0.20, and 0.25. The crystal structure of the a-Ga_2O_3 films under different O_2/Ar flow rate ratios was determined using a Bruker D8 Advance X-ray diffractometer (XRD) with θ-2θ scan mode. The topographic image and surface roughness of the a-Ga_2O_3 films were investigated using a Shimadzu SPM-9700HT atomic force microscope (AFM) in tapping mode. Optical transmittance of the a-Ga_2O_3 films was characterized using a Perkin Elmer Lambda 1050+ UV/Vis spectrophotometer. The wavelength scan range was from 200 nm to 2000 nm. The optical refractive indexes of the a-Ga_2O_3 films were measured by a HORIBA UVISEL PLUS ellipsometer with the wavelength range of 250–1900 nm. X-ray photoelectron spectroscopy (XPS) analysis of the a-Ga_2O_3 films under different O_2/Ar flow rate ratios was conducted using an ESCALAB Xi^+ (Thermo Scientific) system to investigate the chemical bonding states of different a-Ga_2O_3 films.

3 Results and Discussion

3.1 Structure of a-Ga_2O_3 films

Fig. 1a shows XRD patterns of different a-Ga_2O_3 films grown on flexible PI substrates at various O_2/Ar flow rate ratios. Two wide halo peaks around 2θ of 16° and 25° are considered as the representative peaks of flexible PI substrate[22]. Only PI substrate peaks can be observed, indicating the amorphous crystal structure of the Ga_2O_3 films. Fig. 1b presents XRD patterns of different a-Ga_2O_3 films grown on rigid Si substrate at various O_2/Ar flow rate ratios.

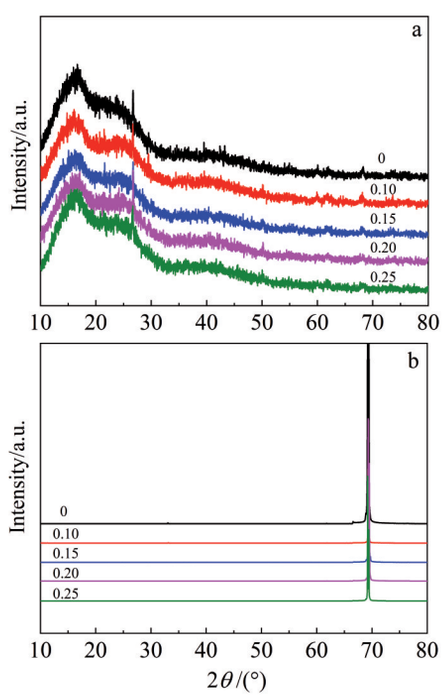

Fig.1 XRD patterns of a-Ga_2O_3 films grown on flexible PI substrate (a) and Si substrate (b) under different O_2/Ar flow rate ratios

There are also no signature peaks, except a sharp peak at around 2θ=69.9°, which originates from single-crystalline Si substrate. These results all confirm the amorphous nature of the a-Ga_2O_3 films. It is known that the crystalline Ga_2O_3 has five polymorphs, among which the β-phase has the most stable monoclinic crystal structure[23–25]. Other phases, no matter metastable or unstable, can be chemically changed into the β-phase at high temperature[23]. The room-temperature deposition and no requirement for crystalline substrates widen the application of a-Ga_2O_3.

XRD patterns of the a-Ga_2O_3 films grown on amorphous PI, quartz glass, and single crystalline Si substrates all exhibit amorphous structure patterns, revealing that the crystal structure of Ga_2O_3 films only depends on the growth temperature instead of the substrate nature or deposition pressure.

3.2 Optical properties of a-Ga_2O_3 films

The wavelength scan range was set from the wavelength of DUV to that of infrared light to investigate the full-spectrum optical properties of a-Ga_2O_3 films. The optical transmittance of the bare PI and quartz glass substrates was also characterized. Fig. 2a shows the full-spectrum optical transmittance of the PI and quartz glass substrates. The erratic fluctuation of the optical transmittance of PI and quartz glass substrates may result from the instability of the spectrometer. On the one hand, the average transmittance of the quartz glass substrate is greater than 90% within the wavelength of 200–2000 nm. On the other hand, the cutoff wavelength of ultraviolet of the flexible PI substrates is about 370 nm, as shown in Fig.2a. It is widely known that the cutoff wavelength of ultraviolet of the a-Ga_2O_3 films should be at approximately 253 nm due to their ultrawide bandgap of about 4.9 eV. Therefore, only the optical transmittance and absorbance of the a-Ga_2O_3 films grown on the quartz glass substrates were measured to eliminate the interference effect from the PI substrates in this research.

The full-spectrum optical transmittance of the a-Ga_2O_3 films deposited on quartz glass substrate under different O_2/Ar flow rate ratios is presented in Fig. 2b. The average transmittance of the a-Ga_2O_3 films grown on quartz glass substrate is greater than 85%. The inset of Fig. 2b demonstrates the optical transmittance spectra of the a-Ga_2O_3 films deposited under different O_2/Ar flow rate ratios within the wavelength from 200 nm to 400 nm. It can be seen that the optical transmittance cutoff edge shows a blueshift phenomenon with the increase in O_2/Ar flow rate ratio from 0 to 0.25. Therefore, the average optical transmittance of the a-Ga_2O_3 films is over 80% within the wavelength range of 300–2000 nm.

Fig.3a shows the absorbance of a-Ga_2O_3 films deposited on quartz glass substrates under different O_2/Ar flow rate ratios. According to Tauc's optical model, the optical band gap of the a-Ga_2O_3 films can be obtained from the following relation[26]:

$$(\alpha h\nu)^2 \propto A(h\nu - E_g) \quad (1)$$

where α is the absorption coefficient, $h\nu$ is the photon energy, A is a constant, and E_g is the optical band gap of the materials. Accordingly, the optical band gap of the a-Ga_2O_3 films can be determined by plotting $(\alpha h\nu)^2$ value versus photon energy $h\nu$

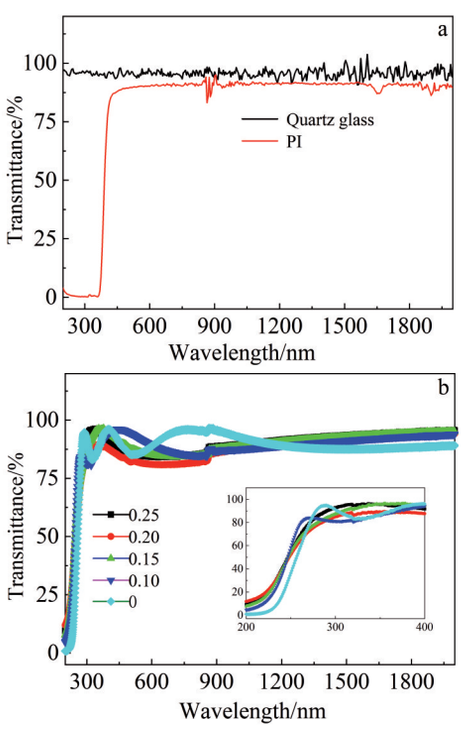

Fig.2 Optical transmittance spectra of bare PI and quartz glass substrates (a) as well as a-Ga_2O_3 films deposited on quartz glass substrates under different O_2/Ar flow rate ratios (b)

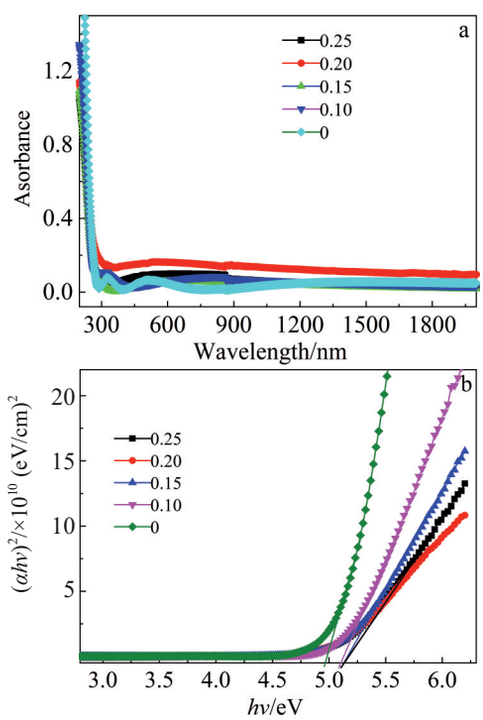

Fig.3 Optical absorbance spectra (a) and $(\alpha h\nu)^2$ curves as a function of $h\nu$ (b) of a-Ga_2O_3 films deposited on quartz glass substrates under different O_2/Ar flow rate ratios

and then fitting the linear region of the plots.

Fig. 3b shows the variation of the $(\alpha h\nu)^2$ as a function of the photon energy $h\nu$ for the a-Ga_2O_3 films grown under different O_2/Ar flow rate ratios. The extracted optical band gap of the a-Ga_2O_3 films is increased from 4.97 eV to 5.13 eV with the increase in O_2/Ar flow rate ratio from 0 to 0.25. The results in Ref. [27–28] showed that the concentration of V_O defects in metal oxide films can be suppressed by increasing the O_2 partial pressure during film growth. The results in Ref. [29–31] also suggested that the intrinsic defects in the form of oxygen vacancies (V_O) behave as donor in the as-grown Ga_2O_3 films. In this research, the optical band gap of the a-Ga_2O_3 films is increased with the increase in O_2/Ar flow rate ratio, which is due to the less presence of oxygen vacancy defects in the electron-hole combination energy state between the conduction and valence band in the a-Ga_2O_3 films. Therefore, oxygen vacancy defects greatly affect the electronic structure and optical energy-band modulation of a-Ga_2O_3 films. Thus, it is important to control the oxygen vacancy concentration to optimize the performance of a-Ga_2O_3-based photodetector devices.

To obtain a comprehensive understanding of the optical properties with varying oxygen vacancies in a-Ga_2O_3 films, the optical refractive index of the a-Ga_2O_3 films deposited under different O_2/Ar flow rate ratios was measured. Fig. 4a and 4b show the refractive index curves of the a-Ga_2O_3 films deposited on quartz glass and Si substrates, respectively. The refractive indexes of the a-Ga_2O_3 films are generally increased as the wavelength decreases into DUV range below 300 nm. Besides,

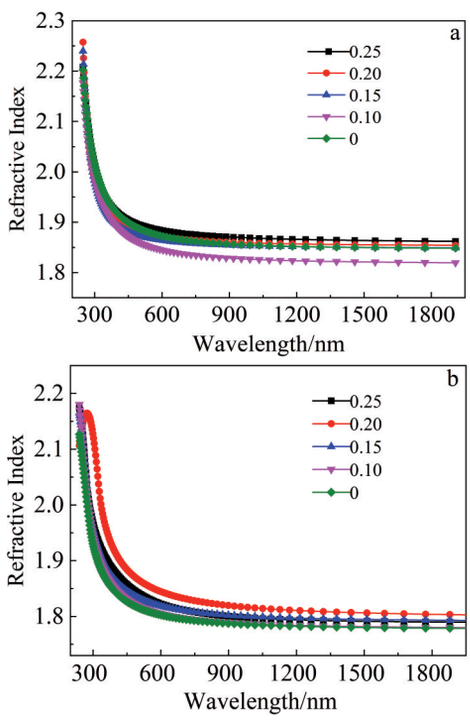

Fig.4 Refractive index curves of a-Ga_2O_3 films deposited on quartz glass substrate (a) and Si substrate (b) under different O_2/Ar flow rate ratios

it is worth noting that the optical refractive index of the a-Ga_2O_3 films is increased with the increase in O_2/Ar flow rate ratio. The concentration of the V_O defects in the a-Ga_2O_3 films is decreased with the increase in O_2/Ar flow rate ratio. Theoretical calculation proposed that the existence of oxygen vacancies can reduce the optical refractive index of yttrium aluminum oxide[32]. The optical refractive index of air (oxygen vacancy) is around 1, which is lower than that of the Ga-O bonding structure. In this research, the decrease in V_O defect concentration with the increase in O_2/Ar flow rate ratio may cause the increase in optical refractive index of the a-Ga_2O_3 films.

3.3 Surface morphology of a-Ga_2O_3 films

Surface morphologies of the a-Ga_2O_3 films grown on Si substrate under different Ar/O_2 flow rate ratios are shown in Fig. 5. The scan area was 5 μm×5 μm for all samples during AFM measurements. For comparison, the surface morphologies of a-Ga_2O_3 films grown on flexible PI and rigid quartz glass substrates were also characterized, as shown in Fig. 6 and Fig. 7, respectively. It is clear that the a-Ga_2O_3 films grown on PI substrate present scratched morphologies and much higher surface roughness. This may result from the deteriorated surface quality of the flexible PI substrates used in this research. On the contrary, the surface morphologies of the a-Ga_2O_3 films deposited on Si and quartz glass substrates present rather smooth characteristics due to their polished surface condition.

Table 1 lists the root mean square (RMS) roughness of the a-Ga_2O_3 films deposited on Si, PI, and quartz glass substrates under different O_2/Ar flow rate ratios. Regardless of the flexible and rigid substrates, RMS roughness of all films is decreased with the increase in O_2/Ar flow rate ratio from 0 to 0.25. Chen et al[33] also reported that the oxygen-rich environment can efficiently reduce the surface structural defects of the Ga_2O_3 films, which is due to the less bombardment of the Ar ions to the film surface under the growth conditions of higher flow rate ratio of oxygen to Ar ratio. Accordingly, the surface oxygen-associated structural defects are greatly suppressed with the increase in O_2/Ar flow rate ratio during the growth of a-Ga_2O_3 films.

Therefore, it is essential to modulate the surface morphology and roughness of the a-Ga_2O_3 films by controlling the oxygen ambient pressure to enhance the performance of the a-Ga_2O_3 films as the active layer for optoelectronic device applications.

3.4 Chemical bonding properties of a-Ga_2O_3 films

Normally, surface chemical bonding states of oxygen atoms can be affected by the ambient pressure during the growth of the oxide films. The stoichiometric ratio in metal-oxide films greatly determines the oxygen-deficient structural defects, which in turn modulates the electrical, optical, and surface properties of the films. Accordingly, the O 1s peak evolution of the a-Ga_2O_3 films with the increase in O_2/Ar flow rate ratio was characterized through XPS measurements to further understand the mechanism of oxygen vacancy defects on the surface chemical bonding state of the a-Ga_2O_3 films. According to XPS analysis results, the binding energy

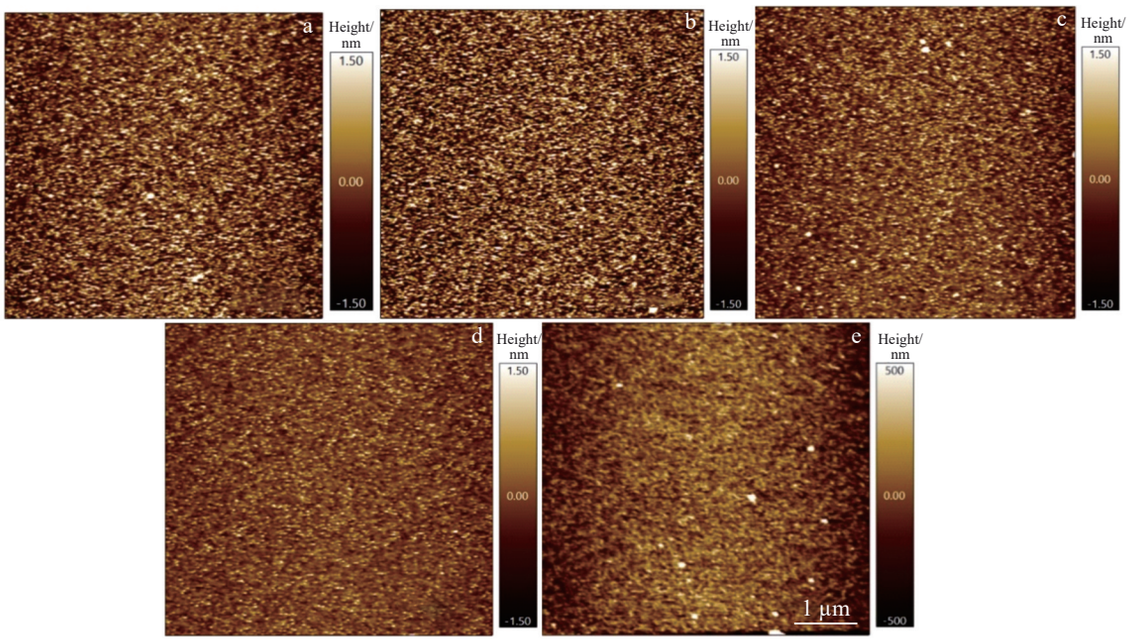

Fig.5 Surface morphologies of a-Ga_2O_3 films deposited on Si substrate under O_2/Ar flow rate ratio of 0 (a), 0.10 (b), 0.15 (c), 0.20 (d), and 0.25 (e)

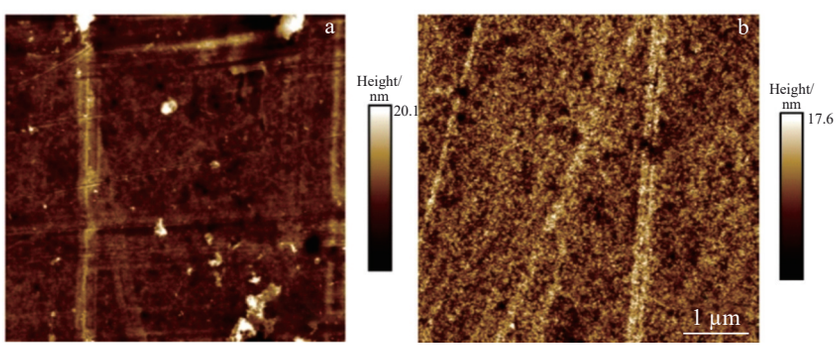

Fig.6 Surface morphologies of a-Ga_2O_3 films deposited on flexible PI substrate under O_2/Ar flow rate ratio of 0 (a) and 0.20 (b)

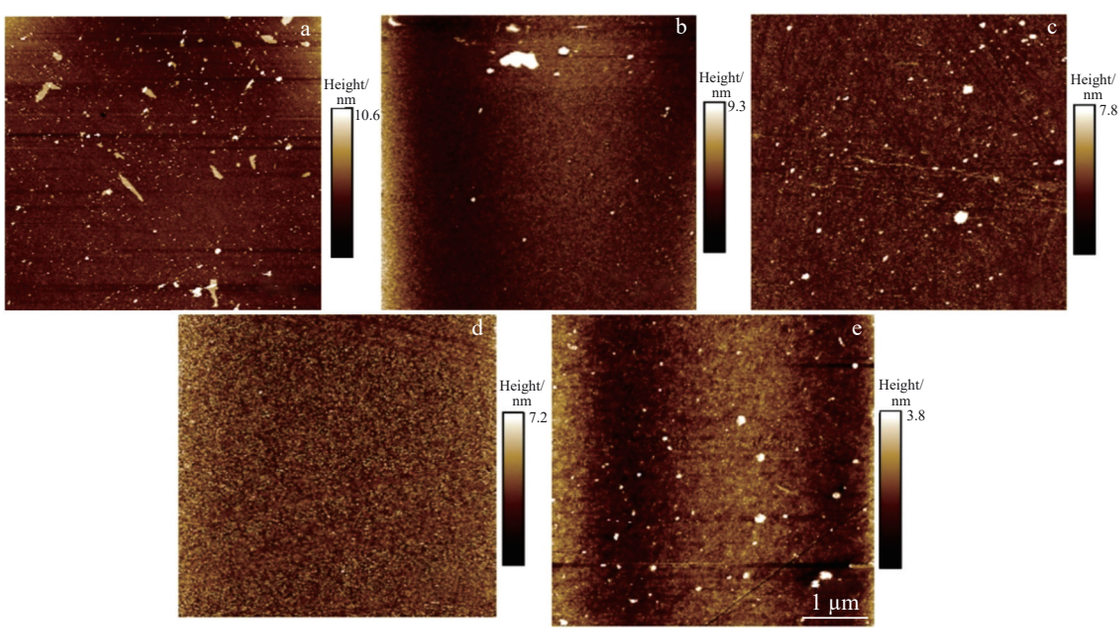

Fig.7 Surface morphologies of a-Ga_2O_3 films deposited on quartz glass substrate under O_2/Ar flow rate ratio of 0 (a), 0.10 (b), 0.15 (c), 0.20 (d), and 0.25 (e)

Table 1 RMS roughness of a-Ga_2O_3 films deposited on Si, PI, and quartz glass substrates under different O_2/Ar flow rate ratios

Deposition substrate	O_2/Ar flow rate ratio	RMS roughness/nm
Si	0	0.59
	0.10	0.64
	0.15	0.48
	0.20	0.32
	0.25	0.25
PI	0	5.18
	0.20	2.45
Quartz glass	0	1.60
	0.10	1.00
	0.15	1.80
	0.20	1.12
	0.25	0.73

referenced to the C 1s is 284.8 eV, which results from adventitious surface carbon contamination. Fig. 8 illustrates XPS spectra of O 1s peak of a-Ga_2O_3 films grown on Si substrate under different O_2/Ar flow rate ratios. It is noticed that the O 1s spectra of the a-Ga_2O_3 films can be divided into three individual peaks using XPS peak fitting program. The peak with lower binding energy of 530.7±0.2 eV corresponds to the oxygen in Ga-O bonding in the a-Ga_2O_3 films. The next peak with higher binding energy of 531.3±0.2 eV corresponds to oxygen in the oxygen-vacancy area in the a-Ga_2O_3 films. The third O 1s peak at around 532.3±0.2 eV is associated with the surface C-O bonds of the a-Ga_2O_3 films[19,34]. Since the origin of the C-O bonds on surface is the surrounding adventitious carbon contamination, the intensity of the O 1s peak of C-O bonding shows little dependence on the O_2/Ar flow rate ratio, as shown in Fig. 8a – 8e. It is clear that the intensity ratio of the V_O peak to Ga-O peak is gradually decreased with the increase in O_2/Ar flow rate ratio from 0 to

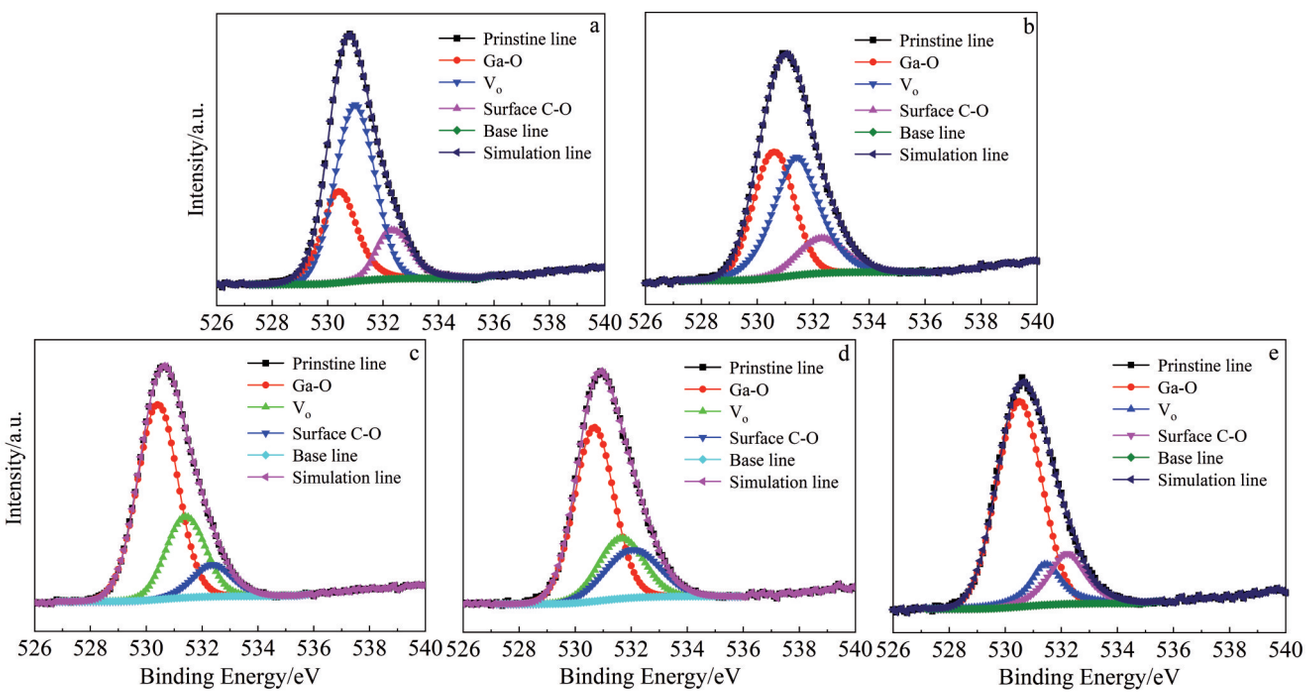

Fig.8 O 1s peak evolution of XPS spectra of a-Ga_2O_3 films deposited on Si substrate under O_2/Ar flow rate ratio of 0 (a), 0.10 (b), 0.15 (c), 0.20 (d), and 0.25 (e)

0.25. These results all demonstrate the suppression effect caused by the concentration of V_O defects with the increase in O_2/Ar flow rate ratio. Therefore, controlling the oxygen partial pressure during growth of the a-Ga_2O_3 films is an essential work in modulation of V_O defect density, which further greatly affects the properties of the a-Ga_2O_3 films and the performance of a-Ga_2O_3-based optoelectronic devices.

4 Conclusions

1) Transparent a-Ga_2O_3 films can be synthesized on flexible PI, rigid quartz glass, and rigid Si substrates via RF magnetron sputtering under different O_2/Ar flow rate ratios at room temperature.

2) The a-Ga_2O_3 films exhibit an average optical transmittance of over 80% from the wavelength of DUV to that of infrared light.

3) The extracted optical band gap of the a-Ga_2O_3 films is increased from 4.97 eV to 5.13 eV with the increase in O_2/Ar flow rate ratio from 0 to 0.25, which is due to the reduction in the oxygen vacancy defects as the donor in the a-Ga_2O_3 films.

4) The optical refractive index of the a-Ga_2O_3 films is increased with the increase in O_2/Ar flow rate ratio.

5) O 1s peak evolution of the a-Ga_2O_3 films deposited under different O_2/Ar flow rate ratios is related to the reduction in the oxygen vacancy defects, which causes the property improvement of a-Ga_2O_3 films.

6) Modulating the oxygen partial pressure during the

a-Ga_2O_3 film growth is important. This research provides a significant reference for future transparent and flexible solar-blind DUV photodetectors.

References

1 Razeghi M. *Proceedings of IEEE*[J], 2002, 90(6): 1006
2 Chen H Y, Liu K W, Hu L F *et al. Materials Today*[J], 2015, 18(9): 493
3 Sang L W, Liao M Y, Sumiya M. *Sensors*[J], 2013, 13(8): 10482
4 Munoz E, Monroy E, Pau J L *et al. Journal of Physics: Condense Matter*[J], 2001, 13(32): 7115
5 Rogalski A, Bielecki Z, Mikolajczyk J *et al. Sensors*[J], 2023, 23(9): 4552
6 Wang H, Jin X L, Chen C P *et al. Chinese Physics B*[J], 2015, 24(3): 038501
7 Jang G, Lee S J, Lee D *et al. Journal of Materials Chemistry C*[J], 2017, 5(18): 4537
8 Huang S Y, Liu Y, Zhao Y *et al. Advanced Functional Materials*[J], 2019, 29(6): 1805924
9 Webb R C, Bonifas A P, Behnaz A *et al. Nature Materials*[J], 2013, 12(11): 938
10 Mahmoud B H, Hexsel C L, Hamzavi I H *et al. Photochemistry and Photobiology*[J], 2008, 84(2): 450
11 Knobelspies S, Daus A, Cantarella G *et al. Advanced Electronic Materials*[J], 2016, 2(10): 1600273
12 Xia S H, Li B M, Yang Z H *et al. Journal of Applied Physics D: Applied Physics*[J], 2023, 56(34): 345105
13 Saha A, Kumar G, Pradhan S *et al. Advanced Materials*[J], 2022, 34(10): 2109498
14 Qi X H, Liu Z, Ji X Q *et al. IEEE Sensors Journal*[J], 2023, 23(3): 2055
15 Qiao P F, Liu K, Dai B *et al. Diamond Related Materials*[J], 2023, 136: 109943
16 Xiao Y, Yang S S, Cheng L Y *et al. Opto-Electronic Engineering*[J], 2023, 50(6): 230005
17 Sui Y, Liang H, Huo W X *et al. Journal of Physics D: Applied Physics*[J], 2020, 53(50): 504001
18 Arora K, Kaur K, Kumar M. *ACS Applied Electronic Materials* [J], 2021, 3(4): 1852
19 Han S, Huang X L, Fang M Z *et al. Journal of Materials Chemistry C*[J], 2019, 7(48): 11834
20 Wang Y H, Li H R, Cao J *et al. ACS Nano*[J], 2021, 15(10): 16654
21 Lany S, Zunger A. *Physics Review Letters*[J], 2007, 98: 045501
22 Zhang Y, Shen L K, Liu M *et al. ACS Nano*[J], 2017, 11(8): 8002
23 Kaur D, Kumar M. *Advanced Optical Materials*[J], 2021, 9(9): 2002160
24 Xu J J, Zheng W, Huang F. *Journal of Materials Chemistry C*[J], 2019, 7(29): 8753
25 Yang Z N, Xu X Y, Wang Y *et al. Applied Physics Letters*[J], 2023, 122(17): 172102
26 Tauc J. *Optical Properties of Solids*[M]. Amsterdam: Elsevier, 1972
27 Wang C Z, Xu D R, Xiao X G *et al. Journal of Materials Science* [J], 2007, 42(23): 9795
28 Liu H N, Zhou P P, Zhang L N *et al. Materials Letters*[J], 2016, 164: 509
29 Polyakov A Y, Nikolaev V I, Yakimov E B *et al. Journal of Vacuum Science and Technology A*[J], 2022, 40(2): 020804
30 Varley J B, Weber J R, Janotti A *et al. Applied Physics Letters*[J], 2010, 97(14): 142106
31 Heinemann M D, Berry J, Teeter G *et al. Applied Physics Letters* [J], 2016, 108(2): 022107
32 Li Tianjing, Wang Lei, He Lin. *Journal of Chengdu University of Information Technology*[J], 2019, 34(2): 216 (in Chinese)
33 Chen Z H, Wang Y S, Zhang N *et al*. *Chinese Physics B*[J], 2023, 32(1): 017301
34 Dupin J C, Gonbeau D, Vinatier P *et al. Physical Chemistry Chemical Physics*[J], 2000, 2(6): 1319

氧气/氩气流量比对柔性和刚性衬底上的非晶Ga_2O_3薄膜性能的影响

李远洁[1]，赵玉清[1]，梁晨煜[2]
(1. 西安交通大学 电子科学与工程学院 电子物理与器件教育部重点实验室，陕西 西安 710049)
(2. 西安交通大学 分析测试中心，陕西 西安 710049)

摘　要：利用射频磁控溅射沉积技术在柔性聚酰亚胺、刚性石英玻璃和硅片衬底上于室温条件下制备了非晶Ga_2O_3薄膜，研究并阐明了氧气/氩气流量比对非晶Ga_2O_3薄膜的结构、光学、表面形貌及化学键结构特性的影响规律。结果表明，非晶Ga_2O_3薄膜在300~2000 nm波长范围内的平均光学透过率大于80%。当非晶Ga_2O_3薄膜生长过程中氧气/氩气流量比从0升高到0.25时，由于薄膜中氧空位缺陷浓度降低，非晶Ga_2O_3薄膜的光学带宽从4.97 eV增加到5.13 eV；非晶Ga_2O_3薄膜的光学折射率和表面粗糙度均随着氧气/氩气流量比达到0.25时最优。同时，X射线光电子能谱测试结果表明，随着氧气/氩气流量比从0升高到0.25，非晶Ga_2O_3薄膜O 1s峰中氧空位和氧-镓化学键的比例逐渐降低，从而证实了升高薄膜生长过程中的氧气/氩气流量比，能够降低非晶Ga_2O_3薄膜中的氧空位缺陷浓度，以获得最优化的非晶Ga_2O_3薄膜性能，为实现高性能的柔性和刚性基于非晶Ga_2O_3薄膜的日盲深紫外探测器件奠定研究基础。

关键词：日盲深紫外探测器；非晶Ga_2O_3薄膜；柔性电子；氧空位缺陷；射频磁控溅射

作者简介：李远洁，女，1974年生，博士，副教授，西安交通大学电子科学与工程学院电子物理与器件教育部重点实验室，陕西 西安 710049，电话：029-82664974，E-mail：liyuanjie@mail.xjtu.edu.cn